Critical behaviour of the fully packed loop model on the square lattice

1996 J. Phys. A: Math. Gen. 29 L399

(http://iopscience.iop.org/0305-4470/29/16/001)

J. Phys. A: Math. Gen. **29** (1996) L399–L404. Printed in the UK

LETTER TO THE EDITOR

Critical behaviour of the fully packed loop model on the square lattice

M T Batchelor†, H W J Blöte‡, B Nienhuis§ and C M Yung†

† Department of Mathematics, School of Mathematical Sciences, Australian National University, Canberra, ACT 0200, Australia

‡ Laboratorium voor Technische Natuurkunde, Technische Universiteit Delft, PO Box 5046, 2600 GA Delft, The Netherlands

§ Instituut voor Theoretische Fysica, Universiteit van Amsterdam, Valckenierstraat 65, 1018 XE Amsterdam, The Netherlands

Received 30 April 1996

Abstract. We investigate the critical behaviour of the fully packed O(n) loop model on the square lattice in which each vertex is visited once by a loop. A transfer-matrix analysis shows that this model can be interpreted as a superposition of a low-temperature O(n) model and an solid-on-solid (SOS) model, as for the fully packed model on the honeycomb lattice. However, not all of the critical exponents are the same for both lattices. In contrast, the fully packed model on the triangular lattice appears to behave as a pure low-temperature O(n) model.

There has been a recent growth of interest in O(n) loop models [1] in the fully packed limit. A loop model is 'fully packed' in the sense that empty vertices are excluded, with every vertex visited once by a loop. Recent work on fully packed loop (FPL) models has been confined to the honeycomb lattice, where exact results have been obtained by a number of authors (see, e.g., [2–6] and references therein). In particular, the FPL model on the honeycomb lattice defines a new universality class characterized by the superposition of a low-temperature O(n) phase and a solid-on-solid (SOS) model at a temperature independent of n [2]. The central charge, thermal and magnetic scaling dimensions are given by [2–6]

$$c^{\mathrm{H}} = 2 - 6(1-g)^2/g \tag{1}$$

$$X^{\mathrm{H}}_{\epsilon} = 3g/2 \tag{2}$$

$$X^{\mathrm{H}}_{\sigma} = 1 - 1/(2g) \tag{3}$$

where $n = -2\cos\pi g$ with $g \in [\frac{1}{2}, 1]$ in the region of interest ($0 \leqslant n \leqslant 2$). The general set of geometric or 'magnetic' scaling dimensions is [5, 6]

$$X^{\mathrm{H}}_{2k-1} = \tfrac{1}{2}g(k^2 - k + 1) - \frac{(1-g)^2}{2g} \tag{4}$$

$$X^{\mathrm{H}}_{2k} = \tfrac{1}{2}gk^2 - \frac{(1-g)^2}{2g} \tag{5}$$

where $k = 1, 2, \ldots$, with $X^{\mathrm{H}}_{\sigma} = X^{\mathrm{H}}_{1}$. These results are to be compared with those of the so-called 'densely packed' loop (DPL) model on the honeycomb lattice, where the O(n)

0305-4470/96/160399+06$19.50

model is in a low-temperature phase [7]. In this case

$$c^{\mathrm{DPL}} = 1 - 6(1-g)^2/g \tag{6}$$

$$X_{\epsilon}^{\mathrm{DPL}} = 3g/2 - 1 \tag{7}$$

$$X_{\sigma}^{\mathrm{DPL}} = 1 - 3g/8 - 1/2g \tag{8}$$

and the geometric dimensions are given by [8]

$$X_{k}^{\mathrm{DPL}} = \tfrac{1}{8}gk^2 - \frac{(1-g)^2}{2g} \tag{9}$$

or $X_{k}^{\mathrm{DPL}} = 2\Delta_{0,k/2}$ in terms of the Kac formula. Here $X_{\sigma}^{\mathrm{DPL}} = X_{1}^{\mathrm{DPL}}$.

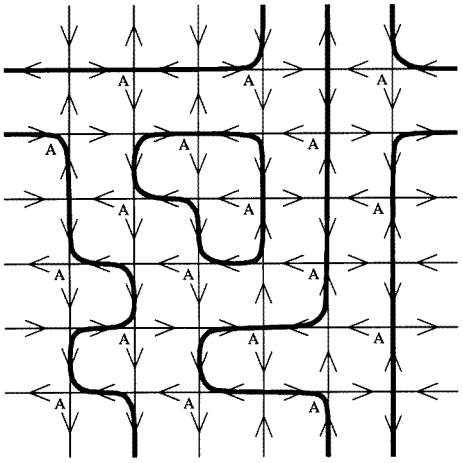

Figure 1. A typical fully packed loop configuration on the periodic square lattice of width $N = 6$. Also shown is the A sublattice and the corresponding six-vertex model configuration for the mapping of the FPL model at $n = 1$ onto the ice model.

In this letter we investigate the FPL model on the square lattice. There are several motivations for this study. First, the FPL model describes Hamiltonian walks in the limit $n = 0$. Hamiltonian walks are self-avoiding walks which visit each site of a given lattice and thus completely fill the available space. They thus describe the configurational statistics of compact or collapsed polymers. At $n = 0$ ($g = \frac{1}{2}$) the above results give $c^{\mathrm{H}} = -1$ and

$$X_{2k-1}^{\mathrm{H}} = \tfrac{1}{4}(k^2 - k) \tag{10}$$

$$X_{2k}^{\mathrm{H}} = \tfrac{1}{4}(k^2 - 1). \tag{11}$$

Thus on the honeycomb lattice the 'compact' exponents, $\nu = \frac{1}{2}$ and $\gamma^{\mathrm{H}} = 1$, follow from $X_1^{\mathrm{H}} = X_2^{\mathrm{H}} = 0$ in the usual way (using $1/\nu = 2 - X_2$ and $\gamma = 2(1 - X_1)\nu$). However, the situation is different for densely packed walks where $c^{\mathrm{DPL}} = -2$ and

$$X_{2k-1}^{\mathrm{DPL}} = -\tfrac{3}{16} + \tfrac{1}{4}(k^2 - k) \tag{12}$$

$$X_{2k}^{\mathrm{DPL}} = \tfrac{1}{4}(k^2 - 1). \tag{13}$$

In this case $\nu = \frac{1}{2}$ and $\gamma^{\mathrm{DPL}} = \frac{19}{16}$†. On the other hand, for Hamiltonian walks on the Manhattan lattice, $\nu = \frac{1}{2}$ and $\gamma^{\mathrm{Man}} = 1$ [11]. It is thus of interest to investigate the

† However, care must be taken in the interpretation of the γ exponents. The DPL value has been interpreted as a difference between walk and polygon extropic exponents rather than the straight walk value [9, 10].

universality of Hamiltonian walks on the square lattice. A further motivation is a mapping of the FPL model onto a SOS model [2, 3, 6, 12] as given below.

The partition function of the FPL model is simply

$$\mathcal{Z} = \sum n^{\mathcal{N}} \tag{14}$$

where n is the fugacity of a closed loop and $\mathcal{N}$ is the total number in a given configuration. The sum is over all configurations of closed and non-intersecting loops on the square lattice, such that every vertex is visited once (see figure 1). There are two types of allowed vertices, representing straight loop segments and 90° turns. Both types have equal weights. We take periodic boundary conditions across a strip of width N and unless indicated otherwise, we take N even. In spite of the non-local weights occurring in the loop model, a transfer matrix can be constructed [13]. The transfer-matrix index is a numeric coding of the way in which the dangling bonds on the surface of the lattice are interconnected by loop segments. The allowed vertex loop configurations are shown in figure 2(a). In general the sectors of the transfer matrix are characterized by the number n_{d} of dangling bonds. The partition sum (14) can also be realized in terms of a local three-state vertex model. The 12 allowed arrow configurations and their corresponding Boltzmann weights are shown in figure 2(b). Here the two phase factors s and s^{-1} are chosen such that $n = s + s^{-1}$ and a seam is introduced in the usual way (see, e.g., [5]) to coincide with the $n_{\mathrm{d}} = 0$ sector.

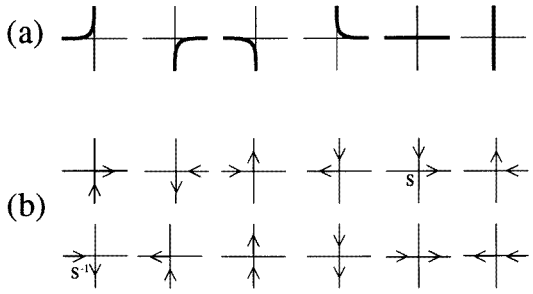

Figure 2. (a) The allowed loop configurations at a vertex. Each vertex has unit Boltzmann weight. (b) The allowed arrow configurations of the corresponding three-state vertex model. Each vertex, apart from the two indicated, has unit weight.

Numerical results

Unlike the FPL model on the honeycomb lattice, the square lattice model does not appear to be exactly solvable. Nevertheless, accurate estimates of the central charge and scaling dimensions can be obtained via the transfer matrix eigenvalues. In particular, the largest eigenvalue λ_0 determines the finite-size free energy via $f_N = N^{-1} \log \lambda_0$ with [14, 15]

$$f_N \simeq f_\infty + \frac{\pi c}{6N^2} \tag{15}$$

where f_∞ is the bulk free energy and c is the central charge. On the other hand, the scaling dimensions X_i are related to the inverse correlation lengths via [16]

$$\xi_i^{-1} = \log(\lambda_0/\lambda_i) \simeq 2\pi X_i/N. \tag{16}$$

Estimates of c obtained with the loop model transfer matrix are shown in table 1. They agree with the result (1) for the honeycomb model. These results were based on even system sizes $L = 2, 4, \ldots, 14$. A similar analysis on odd systems $L = 3, 5, \ldots, 15$ yielded the

amplitude c^{odd} also shown in the table. Its difference with c appears to be $\frac{3}{2}$ for all n values. This constant is interpreted as a scaling dimension $X = \frac{1}{8}$ (compare the factor 12 between the amplitudes appearing in equations (15) and (16). The table further includes estimates for X_ϵ (obtained from the second largest translationally invariant eigenvalue) and X_1 (obtained from the largest eigenvalue in the sector with one extra 'string' spanning the length of the cylinder, and corresponding with the spin–spin correlation function). Furthermore, similar results for X_2 (obtained in the sector with two additional O(n) strings) are shown. Both X_ϵ and X_1 are clearly different from the honeycomb case. However, X_2 appears to be equal to $X_1^{\mathrm{H}} = X_2^{\mathrm{H}}$ of the honeycomb model. It seems most likely that the 'even' set of geometric dimensions is shared between the various models, with $X_{2k} = X_{2k}^{\mathrm{H}} = X_{2k}^{\mathrm{DPL}}$. We thus see the universal value $\nu = \frac{1}{2}$ at $n = 0$. However, the 'odd' set of dimensions differ, just as $X_{2k-1}^{\mathrm{H}} \neq X_{2k-1}^{\mathrm{DPL}}$. This has significant implications for Hamiltonian walks on the square lattice, where it follows at $n = 0$ that $\gamma \simeq 1.0444$. This result is to be compared with the values $\gamma^{\mathrm{H}} = 1$, $\gamma^{\mathrm{DPL}} = \frac{19}{16}$ and $\gamma^{\mathrm{Man}} = 1$. This configurational exponent is thus particularly sensitive to the details of the underlying lattice. From table 1 it appears that $X_1^{\mathrm{odd}} = X_1^{\mathrm{DPL}}$. Moreover, our numerical estimates of the dimension X_3 are indicative of the value $X_3 = X_1 + g$. However, we have not been able to make a convincing guess for the exact values of the odd scaling dimensions and thus the exact value of the exponent γ.

Table 1. Numerical results for the central charge c and various scaling dimensions X_i from an analysis using both even and odd system sizes. Corresponding exact results for the honeycomb FPL and DPL models are also shown below for comparison.

n	c	c^{odd}	X_1	X_2	X_ϵ	X_1^{odd}
0.0	−1.00(1)	−2.4977(2)	−0.0444(1)	0.000 00(0)	0.573(1)	−0.1874(1)
0.5	0.180(5)	−1.3188(2)	0.0750(3)	0.138 60(2)	0.6200(5)	−0.0790(1)
1.0	1.000(1)	−0.5000(1)	0.1667(1)	0.250 0(1)	0.6666(1)	0.0000(0)
1.5	1.59(1)	0.087(5)	0.242(2)	0.350(1)	0.713(1)	0.0616(2)
2.0	2.00(1)	0.500(2)	0.307(2)	0.46(2)	0.76(1)	0.114(5)
n	$c^{\mathrm{H}} = c^{\mathrm{DPL}}+1$	$c^{\mathrm{H}} - \frac{3}{2}$	$X_1^{\mathrm{H}} = X_2^{\mathrm{H}}$	$X_2^{\mathrm{H}} = X_2^{\mathrm{DPL}}$	$X_\epsilon^{\mathrm{DPL}}$	X_1^{DPL}
0.0	−1	−2.5		0	−0.25	−0.1875
0.5	0.180	−1.320		0.1386	−0.129	−0.0791
1.0	1	−0.5		0.25	0	0
1.5	1.588	0.088		0.3506	0.155	0.0619
2.0	2	0.5		0.5	0.5	0.125

Exact results at $n = 1$

Some exact information can be obtained for the FPL model at $n = 1$ via a mapping onto the ice model. We first divide the lattice sites into two sublattices A and B (see figure 1). Then, a loop-line passing through an A site is represented by incoming arrows on the A sites, which are outgoing arrows on the B sites. Conversely, the opposite situation pertains to the empty bonds—with incoming arrows on B sites and outgoing arrows on A sites. This gives a one-to-one correspondence between the loop configurations of the FPL model at $n = 1$ and the arrow configurations of the six-vertex ice model [17]. However, the correspondence between eigenvalues in the transfer matrix eigenspectra is only partial. The loop transfer matrix carries some redundant information at $n = 1$ because the way in which the loop segments are interconnected is irrelevant. Thus, we expect that the eigenspectrum of the loop transfer matrix contains extra eigenvalues which are associated with geometric properties of the loops, and do not contribute to the thermodynamics. We observe that the

largest eigenvalue of the FPL model coincides with the largest eigenvalue of the ice model. It immediately follows that the bulk free energy is given by $f_\infty = \frac{3}{2}\log\frac{4}{3}$ and, moreover, that the central charge is $c = 1$. The eigenvalues associated with the magnetic and thermal scaling dimensions are seen to respectively coincide with the leading eigenvalues in the next-largest and next-next-largest sectors of the ice model transfer matrix. These eigenvalues are known to have scaling dimensions $X_m = m^2 x_p$, where $m = 1, 2$ and $x_p = \frac{1}{6}$ for the ice model [18]. Thus $X_\sigma = \frac{1}{6}$ and $X_\epsilon = \frac{2}{3}$ at $n = 1$. We have observed that, at least for the small sizes we could treat, all eigenvalues of the ice-model transfer matrix occur in the eigenspectra of the O(1) model. Thus the latter must contain as a subset all scaling dimensions of the former, namely $X_{m,p} = \frac{1}{6}m^2 + \frac{3}{2}p^2$.

Table 2. Numerical results for the central charge c of the FPL model on the triangular lattice. Unlike the honeycomb and square models, the results agree with pure low-temperature O(n) behaviour. The exact central charge in the DPL phase is shown for comparison.

n	c	c^{DPL}
0.0	−2.00(1)	−2
0.5	−0.81(1)	−0.820
1.0	0.00(1)	0
1.5	0.59(1)	0.588
2.0	1.000(5)	1

Entropy at $n = 0$

We have estimated the free energy density at $n = 0$, namely $f_\infty = 0.387\,165(1)$, on the basis of even system sizes up to $L = 16$, and $0.387\,164(1)$ from odd sizes up to $L = 15$. These results are a refinement on earlier values [19–21]. An estimate for the 'entropy' loss per step due to compactness, relative to the freedom of open configurations, follows as $f_\infty - \log\mu = -0.5829$ (cf [21]), where $\mu = 2.638\,16$ for self-avoiding walks on the square lattice [22]. The corresponding quantity is known exactly, $-0.4831\ldots$, on the honeycomb lattice [5].

SOS interpretation

In analogy with the honeycomb case, one may interpret the square FPL model as a multi-component SOS model. One SOS component can be defined as the BCSOS variable associated with the six-vertex representation. Another SOS variable can be obtained by viewing the loops as domain walls between regions in which this variable changes by one unit. The sign of the step can be taken from the direction of the arrow in the vertex representation as depicted in figure 2(b). Obviously only when $n = 2$ are the weights of these SOS configurations all the same and equal to one.

The triangular FPL model

A similar FPL model (equation (14)) can be defined on the triangular lattice by requiring that each vertex is visited precisely once by a loop and that all allowed vertices have the same weight. Transfer-matrix calculations were performed using finite sizes up to $L = 7$. We have estimated the free energy density at $n = 0$ to be $f_\infty = 0.7395(5)$. Thus taking the value $\mu = 4.150\,76$ for self-avoiding walks on the triangular lattice [23], the 'entropy' loss is $\simeq -0.6838$. The finite-size dependence of the free energy was analysed according to equation (15). The results for the central charge are shown in table 2. They are obviously different from those of the honeycomb and square models (see, e.g., table 1). Instead, the triangular model appears to behave as a low-temperature O(n) model. This phenomenon

can be related to the fact that loops covering an odd number of bonds occur in the triangular FPL model. Since such loops are absent in the honeycomb and square O(n) models, these models are invariant under a change of sign of the weight of the empty vertex. Then, the FPL models are cases of special symmetry leading to the appearance of new universal behaviour [2]. This symmetry is absent in the triangular FPL model.

It is a pleasure to thank Aleks Owczarek for some helpful comments. This work has been supported by the Australian Research Council and the 'Stichting voor Fundamenteel Onderzoek der Materie (FOM)' which is financially supported by the 'Nederlandse Organisatie voor Wetenschappelijk Onderzoek (NWO)'.

References

[1] Domany E, Mukamel D, Nienhuis B and Schwimmer A 1981 *Nucl. Phys.* B **190** 279
[2] Blöte H W J and Nienhuis B 1994 *Phys. Rev. Lett.* **72** 1372
[3] Kondev J and Henley C L 1994 *Phys. Rev. Lett.* **73** 2786
[4] Blöte H W J and Nienhuis B 1994 *Phys. Rev. Lett.* **73** 2787
[5] Batchelor M T, Suzuki J and Yung C M 1994 *Phys. Rev. Lett.* **73** 2646
[6] Kondev J, de Gier J and Nienhuis B 1996 *Preprint* cond-mat/9603170
[7] Nienhuis B 1987 *Phase Transitions and Critical Phenomena* vol 11, ed C Domb and J L Lebowitz (London: Academic)
[8] Duplantier B 1986 *J. Phys. A: Math. Gen.* **19** L1009
[9] Duplantier B 1993 *Phys. Rev. Lett.* **71** 4274
[10] Owczarek A L, Prellberg T and Brak R 1993 *Phys. Rev. Lett.* **71** 4275
[11] Batchelor M T, Owczarek A L, Seaton K A and Yung C M 1995 *J. Phys. A: Math. Gen.* **28** 839 and references therein
[12] Huse D A and Rutenberg A D 1992 *Phys. Rev.* B **45** 7536
[13] Blöte H W J and Nienhuis B 1989 *J. Phys. A: Math. Gen.* **22** 1415
[14] Blöte H W J, Cardy J L and Nightingale M P 1986 *Phys. Rev. Lett.* **56** 742
[15] Affleck I 1986 *Phys. Rev. Lett.* **56** 746
[16] Cardy J L 1984 *J. Phys. A: Math. Gen.* **17** L385
[17] Lieb E H 1967 *Phys. Rev.* **162** 162
[18] Alcaraz F C, Barber M N and Batchelor M T 1988 *Ann. Phys., NY* **182** 280 and references therein
[19] Orr W J C 1947 *Trans. Faraday Soc.* **43** 12
[20] Schmalz T G, Hite G E and Klein D J 1984 *J. Phys. A: Math. Gen.* **17** 445
[21] Chan H S and Dill K A 1989 *Macromol.* **22** 4559
[22] Guttmann A J and Enting I 1988 *J. Phys. A: Math. Gen.* **21** L165
[23] Guttmann A J 1987 *J. Phys. A: Math. Gen.* **20** 1839